Check for updates

# Trough cross-bedded rhodolith limestones in the Atlantic-linked Ronda Basin (Messinian, Southern Spain)

Juan C. Braga* and Julio Aguirre

Dpto Estratigrafía y Paleontología, Facultad de Ciencias, Fuentenueva s/n, Universidad de Granada, Granada, Spain

Rhodolith limestones occur in the upper part of the Miocene infill of the Ronda Basin in southern Spain. This basin was an embayment at the southern margin of the Atlantic-linked Guadalquivir Basin, the foreland basin of the Betic Cordillera. Messinian rhodolith limestones crop out in the mesa of the Roman settlement Acinipo. They mostly consist of trough cross-bedded rhodolith rudstones, which change basinward to large-scale planar cross-bedded rhodolith rudstones, which in turn pass laterally to planar cross-bedded and flat-bedded bryozoan rudstones. Rhodoliths in rudstones are generally broken, exhibiting several phases of breakage and restarted growth of coralline algae. Many rhodoliths also show asymmetrical growth. The rudstone matrix is a packstone with fragments of coralline algae, bryozoans, calcitic bivalves, echinoids, and foraminifers. Large lithoclasts from the basement, heavily bored by bivalves, are common in the rhodolith rudstone, especially in the most massive type. Rhodolith characteristics and sedimentary structures suggest that trough cross-bedded rhodolith rudstones accumulated in submarine dunes moved by storm surges in a littoral wedge at the western side of a small bay (the Ruinas de Acinipo bay) in the Ronda Basin. Large-scale planar cross-bedded coralline algal and bryozoan rudstones formed in the foresets of the wedge progradation below the storm-wave base. The dominance of Lithophyllaceae and Hapalidiales, with scarce representatives of Corallinaceae in the coralline algal assemblages, reflects that Ronda and Guadalquivir basins opened to the Atlantic Ocean.

## 1 Introduction

Fossil rhodolith concentrations formed on gently dipping ramps and rimmed shelves usually are massive or roughly bedded deposits of decimeters to several meters thickness (Pisera and Studencki, 1989; Aguirre et al., 1993, 2012, 2017; Nalin et al., 2008; Brandano et al., 2009; Bassi and Nebelsick, 2010; Brandano and Piller, 2010; Cornée et al., 2012; Brandano and Ronca, 2014; Brandano, 2017; Sola et al., 2022). This reflects

autochthonous to parautochthonous accumulation of rhodoliths growing under low to moderate hydrodynamic conditions and low sediment supply for prolonged times (Aguirre et al., 2017 and references therein; Millar and Gagnon, 2018). Rhodolith concentrations also occur in large-scale cross beds or clinoforms on the slope of platforms, such as in the early Miocene of Sardinia (Benisek et al., 2009, 2010) or on the steeply inclined distal part of ramps, such as in the Late Miocene ramp in Menorca (Obrador et al., 1992; Pomar, 2001; Pomar et al., 2002; Brandano et al., 2005) and in the foresets of a littoral wedge in the Miocene of Corsica (Brandano and Ronca, 2014). The clinoforms reflect a steep depositional profile on which *in situ* rhodolith growth was as important as downslope displacement of coralline nodules from shallower areas. In contrast, trough cross-bedded dense rhodolith accumulations have only been described in short intervals in rhodolith limestones mainly displaying massive to crude bedding or channelized beds (Miocene of Malta, Bosence and Pedley, 1982; Oligocene of Malta and southern Italy, Pedley, 1998; Pliocene of Guadeloupe, Cornée, et al., 2012). The trough cross-bedded intervals probably represent the shallowest facies of middle-ramp rhodolith concentrations (Pedley, 1998; Cornée et al., 2012).

At first sight, trough-cross bedding generated in submarine dunes seems incompatible with *in situ* rhodolith growth, which is usually favored by low to moderate turbulence. However, despite the rarity of reported cases in the geological record, rhodoliths might grow on submarine dunes and be incorporated into them if the frequency of dune reactivation is low enough to allow the slow-growing coralline algae to develop on nodule surfaces between events of dune movement (Testa and Bosence, 1998, 1999).

Here, we describe a cross-bedded rhodolith limestone, up to 20 m thick, which forms a mesa on which the Roman town of Acinipo was settled. This limestone is part of the infill of the Ronda Basin, a Neogene basin at the southern margin of the Atlantic-linked Guadalquivir Basin in southern Spain. We show that rhodoliths grew on submarine dunes in a sheltered bay episodically affected by storms.

The main objectives of this study were: 1) to characterize the facies comprising the rhodolith limestone in Acinipo; 2) to identify the size, shape, internal structure, and components of the rhodoliths; 3) to develop a paleoenvironmental model for rhodolith growth and facies development; and 4) to compare the coralline algal assemblages in the Ronda Basin with coeval assemblages in the western Mediterranean.

## 2 Geological setting

The rhodolith limestone occurs in the upper part of the Miocene sedimentary infill of the Ronda Basin, which was a marginal basin at the southern margin of the Guadalquivir Basin,

the foreland basin of the Betic Cordillera (Figure 1A). This cordillera is the westernmost segment of the Alpine peri-Mediterranean orogenic belt. The Guadalquivir Basin is an elongated foreland basin (Figure 1A), which developed during the late Miocene in response to flexural subsidence of the southern Iberian margin. The subsidence was caused by the stacking of thrust units at the front of the Betic Cordillera during the latest stages of its building (Fernàndez et al., 1998; García-Gastellanos et al., 2002; Iribarren et al., 2009; Vergés and Fernàndez, 2012; Barnolas et al., 2019). The successive closure of the Betic straits from the early Tortonian to the early Messinian due to the uplift of the Betic mountains isolated the Guadalquivir Basin from the Mediterranean Sea (Martín et al., 2001, 2009, 2014; Betzler et al., 2006; Puga-Bernabeu et al., 2022). Since the early Messinian, the basin was only open to the Atlantic Ocean (Martín et al., 2014).

Like other small basins at the active southern margin of the Guadalquivir Basin, the Ronda Basin evolved as a depocenter surrounded by actively uplifting uplands, which fed the basin deposits with terrigenous sediments. The stratigraphic models for the Miocene infill of the basin proposed by various authors differ in several aspects (Bourgois, 1978; Serrano, 1979; Rodríguez-Fernández, 1982; Gläser and Betzler, 2002; Ruiz-Constán et al., 2009). However, they agree on the occurrence of lower Tortonian conglomerates, sands, and silts, which lie unconformably over the basement and change laterally to terrigenous packstones and marls. These deposits are overlain by upper Tortonian terrigenous packstones, and Messinian terrigenous packstones to rudstones, both grading basinward into marls and silty marls. The thickness of the marine sedimentary infill in this basin is irregular and may attain 300 m (Ruiz-Constán et al., 2009). Gläser and Betzler, (2002) suggest facies partitioning due to the irregular relief of the basin, conditioned by folds active at least since the Late Miocene (Balanyá et al., 2007; Galindo-Zaldívar et al., 2019). Embayments in the complex paleogeography were protected from the terrigenous influx and favored carbonate deposition. The Acinipo rhodolith concentration formed in one of these carbonate bays in the northwestern part of the basin (Gläser and Betzler, 2002).

## 3 Methods

Eight sections (ACI 1–8) were logged along the western and northern sides of the Acinipo outcrop (Figure 1B), and additional observations were made at exposed points at the generally covered eastern side (Figure 2). Another section was logged at the ACI 9 outcrop located 1.8 km to the southeast (Figure 1B). Lithofacies characterization and component identification in the field were completed with optical microscopy analysis of 38 thin sections cut from selected rock samples.
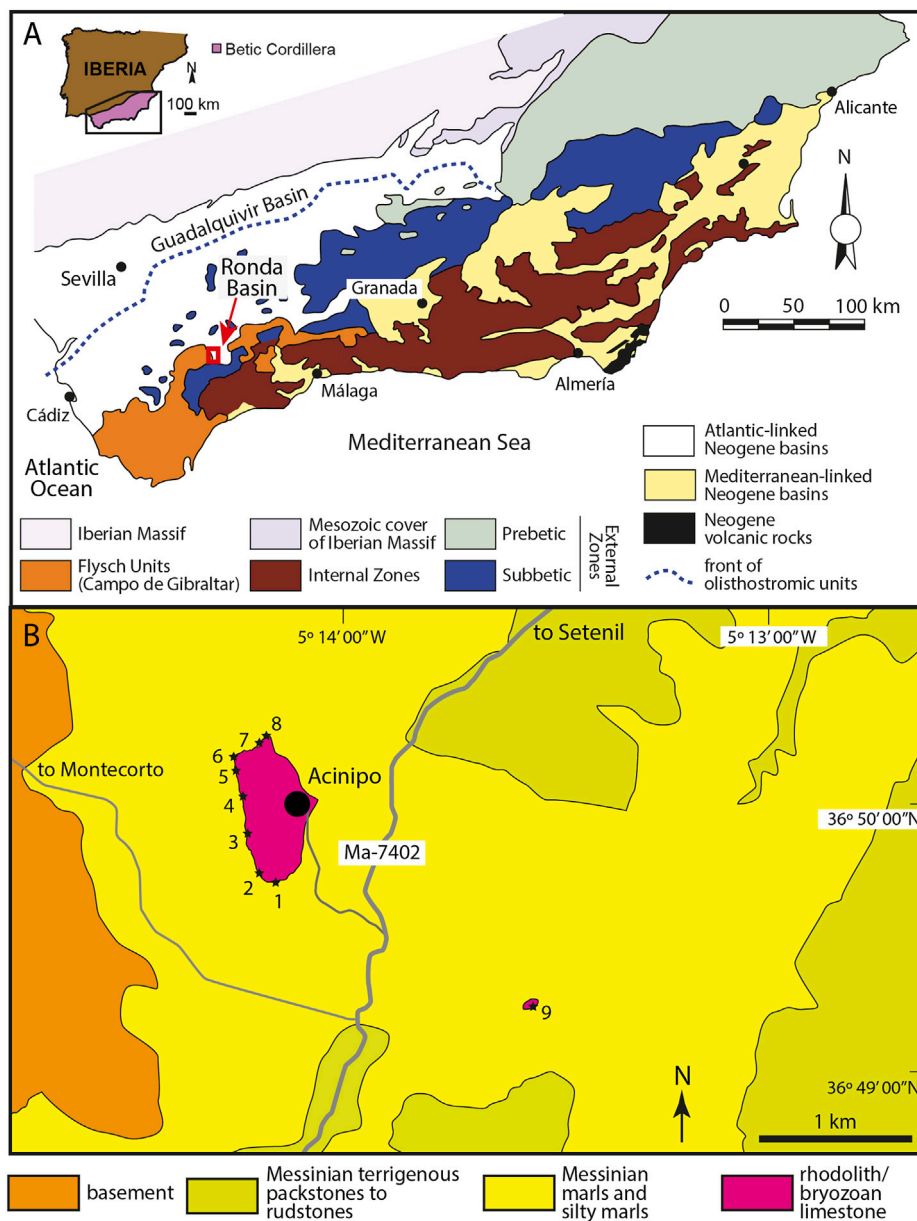
**FIGURE 1**
**(A)** Location of the Ronda Basin at the southern margin of the Guadalquivir Basin, the foreland basin of the Betic Cordillera in southern Spain. Red rectangle indicates the location of **(B)**. **(B)** Access roads and lithological map of the Acinipo area with the location of study sections (black stars 1−9).

The size and shape of rhodoliths were examined in 2D sections at the outcrops, as the extraction of isolated rhodoliths was impossible due to limestone cementation. The internal arrangement, algal growth form, and algal composition of rhodoliths were analyzed both at the outcrop and in thin sections. We use the terminology proposed by Woelkerling et al. (1993), as well as the recent terminology updated by Aguirre et al. (2017). Coralline algae were identified at the most precise taxonomic level possible, in most cases identifying the (morpho)species group, i.e., identifying the living or fossil species whose morpho-anatomical diagnostic characters can be observed in the fossil specimens. When identified species could not be confidently assigned to a previously described one, an open specific nomenclature was applied. The taxonomic

**FIGURE 2**
Representative columns of study sections (see Figure 1B for location).
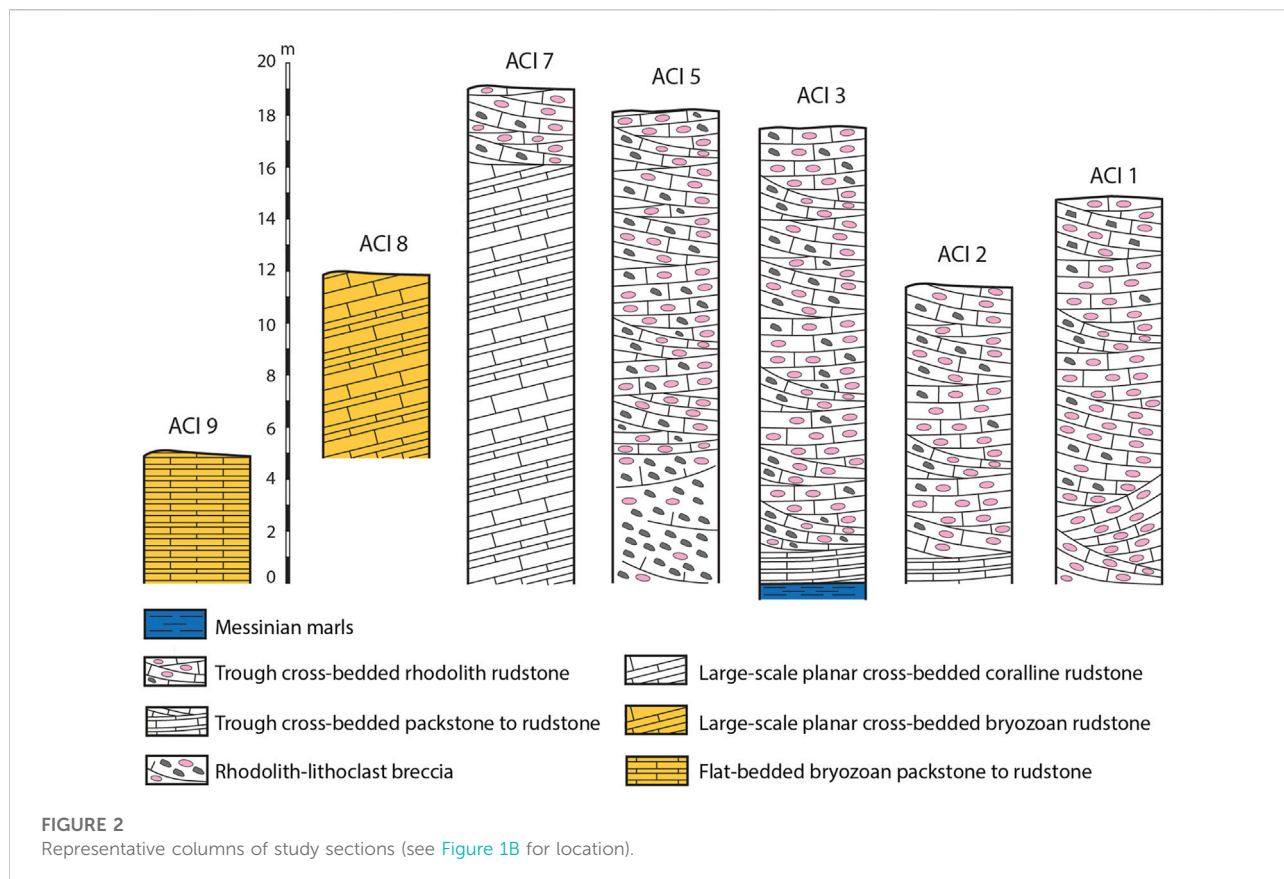
scheme of orders, families, subfamilies, and genera follows recent molecular phylogenies (Peña et al., 2020; Jeong et al., 2021).

The age of marls underlying the rhodolith limestone was defined by analyzing planktonic foraminifer and calcareous nannoplankton assemblages. To extract planktonic foraminifers, two marl samples were washed using meshes, and the residue in the 0.125 mm fraction was examined. For calcareous nannoplankton, two smeared slides of sediment were prepared and examined looking for the biostratigraphically significant species.

# 4 Results

## 4.1 Age

The Acinipo rhodolith limestone unconformably overlies marls attributable to the early Messinian based on the dominance of the *Globorotalia miotumida* group (Sierro, 1985; Lirer et al., 2019) in the planktonic foraminifer assemblages and the presence of *Amaurolithus amplificus*, a calcareous nannoplankton species first occurring in the early Messinian (Martini, 1971; Okada and Bukry, 1980; Young et al., 1994; Raffi and Flores, 1995).

## 4.2 Lithofacies

The following lithofacies were distinguished based on field observations and microscopic analysis of thin sections (Figures 3–6).

### 4.2.1 Trough cross-bedded rhodolith rudstone

The rudstone consists of rhodoliths, most of them broken, and coralline algal debris (Figures 3A–C), fragments of bryozoans, echinoids, bivalves (oysters and pectinids), serpulids, benthic (larger and small) and planktonic foraminifers, and terrigenous grains (quartz and carbonates). Rhodoliths are either randomly oriented or locally at the base of beds, with their long axes parallel to bedding. The identifiable benthic foraminifers belong to *Amphistegina*, *Elphidium*, and *Sphaerogypsina*. Large lithoclasts (centimeters to a few decimeters in size) of marl and marly limestone occur dispersed in the rudstone in varying proportions. Nearly all lithoclasts are bored by bivalves; the boring traces (*Gastrochaenolites*) are differentially preserved and stand out in the voids left by erosion of the marly lithoclasts (Figure 3D). Rhodoliths and other skeletal components are also bored by bivalves, sponges (*Entobia*), and polychaetes (*Trypanites*). The intergranular spaces are partially filled by a wackestone to
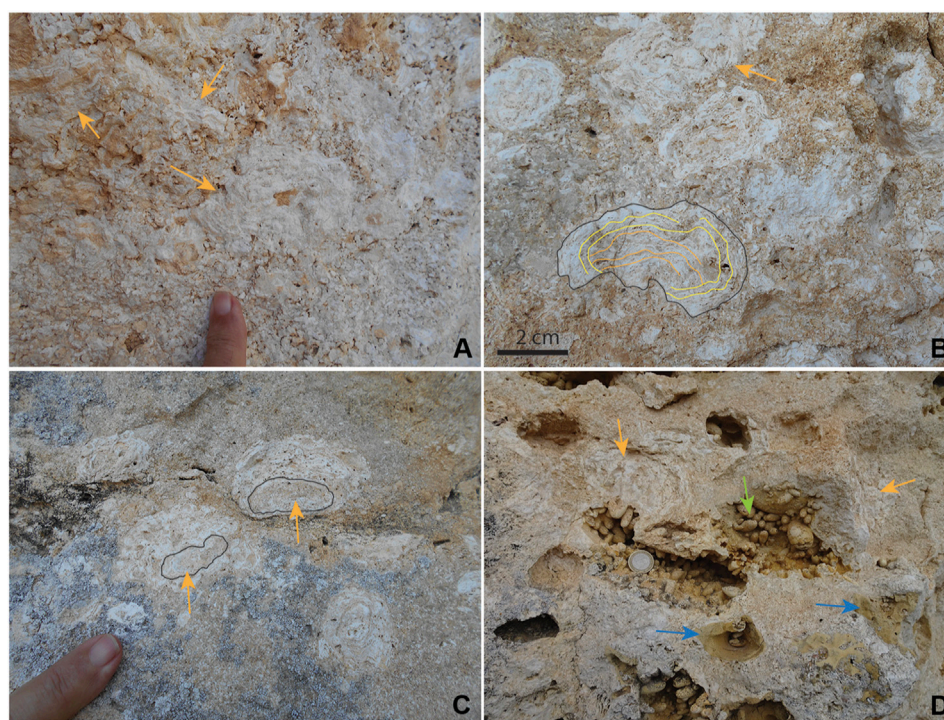
**FIGURE 3**
Field pictures of rhodoliths and lithoclasts in the Acinipo limestone. **(A)** Broken rhodoliths (arrows) in the trough cross-bedded rhodolith rudstone. Maximum finger width is 2 cm. **(B)** Broken rhodolith (arrow) and rhodolith with three phases of growth and fragmentation outlined in the trough cross-bedded rhodolith rudstone. **(C)** Asymmetrical rhodoliths with an initial growth phase outlined (arrows) in the trough cross-bedded rhodolith rudstone. Maximum finger width is 2 cm. **(D)** Broken rhodoliths (orange arrows) and lithoclasts in the massive rhodolith−lithoclast rudstone. Some lithoclasts partly preserve the original marly limestone composition (blue arrows). In most cases, the original marly limestone is leached/eroded, and only *Gastrochaenolites* borings filled with rudstone/packstone are preserved (green arrow). The coin diameter is 2.3 cm.

packstone matrix, whose distribution is irregular. The remaining space among bioclasts and terrigenous grains and intraskeletal voids are partially to totally filled by sparry calcite cement. The rudstone beds are roughly defined, centimeters to decimeters thick, arranged in troughs of decimeters to several meters (up to 5 m) high and several tens of meters long (Figure 4). Only three trough axes were observed, indicating a northward direction of migration (N5-12E). Most of the bed sets also indicate northward migration, but others dip eastward and southward.

## 4.2.2 Trough cross-bedded packstone to rudstone

The components of this facies are fragments of coralline algae, bryozoans, echinoids, bivalves (oysters and pectinids), serpulids, benthic (larger and small) and planktonic foraminifers, and terrigenous grains, mainly quartz (Figure 5A). Broken rhodoliths and marly lithoclasts appear dispersed in the rudstone. The matrix is made of wackestone to mudstone (Figure 5A). Intraskeletal and interskeletal voids are filled by sparry calcite. This facies occurs as thin (3–5 cm)

packstone beds alternating with thicker (10–20 cm) beds of rudstone, both in troughs decimeters high and a few tens of meters long.

## 4.2.3 Massive rhodolith−lithoclast rudstone

This facies consists of a mixture of broken rhodoliths and marly lithoclasts, up to 30 cm in size (Figure 3D), with a matrix of composition like that of trough cross-bedded packstone to rudstone. It occurs in the lower part of the ACI 5 section as a roughly trough cross-bedded, lens-shaped body up to 5 m thick (Figure 2).

## 4.2.4 Large-scale planar cross-bedded rudstone

This facies occurs at the northern extreme of the Acinipo outcrop (Figures 1B, 2). The rudstone beds, centimeters to a few decimeters thick, are arranged in large-scale, planar cross-beds, dipping 15–20° to the east (N80-90E). The bed sets are decimeters to meters thick (Figure 6). There are two subfacies depending on the main component.

Coralline algal rudstone. This subfacies is composed of bioclasts of coralline algae, bryozoans, echinoids, bivalves
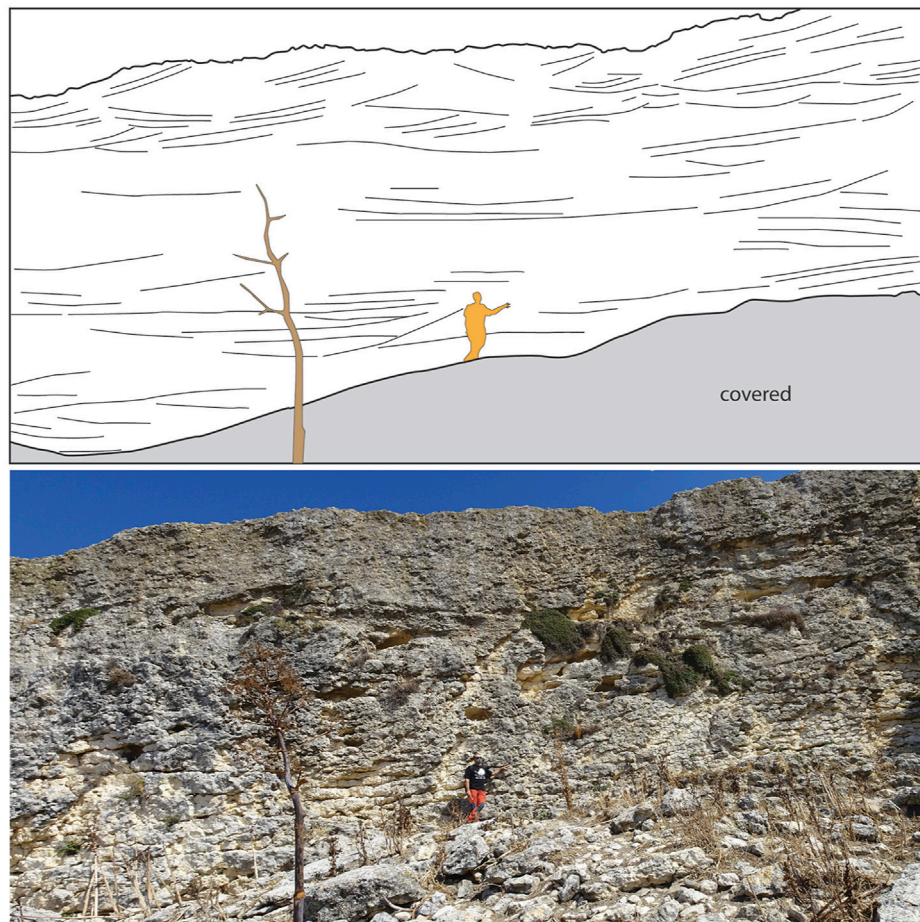
**FIGURE 4**
View of the trough cross-bedded rhodolith rudstone between Sections 1, 2. The drawing in the upper panel remarks the most outstanding bedding surfaces. Note the poorly defined cross-bedding with most troughs pointing to the north (into the wall and to the left).

(oysters, pectinids, and molds of aragonitic taxa), benthic (larger and small) and planktonic foraminifers, and terrigenous grains, mainly quartz. The matrix is a mudstone to wackestone (Figure 5B). Intraskeletal and interskeletal voids, and molds of aragonitic bivalves are filled by sparry calcite.

Bryozoan rudstone. Bryozoans are the main components in this subfacies with subordinate coralline algae. The rest of the components, matrix, and cement are like those of the coralline algal subfacies, although aragonitic bivalves are scarce (Figure 5C).

### 4.2.5 Flat-bedded bryozoan packstone to rudstone

Bryozoans are the main components of this facies (Figure 5D) with accessory coralline algae, echinoids, pectinids, serpulids, small benthic and planktonic foraminifers, and quartz grains. The matrix is a mudstone to wackestone. Inter- and intraskeletal voids are filled with sparry calcite.

This facies occurs as alternating thin (a few centimeters) packstone and thicker (up to 20 cm) rudstone beds only in section ACI 9 (Figure 2) separated from the main Acinipo outcrop (Figure 1B). The bedding surfaces show a wavy geometry probably diagenetic in origin.

## 5 Sections

Trough cross-bedded rhodolith rudstone (Figures 3A–C, 4) is the single or the predominant lithofacies in sections at the southern and western margins of the outcrop (Figures 1B, 2). Trough cross-bedded packstone to rudstone occurs at the base of the southwestern sections, and the rhodolith–lithoclast breccia (Figure 3D) appears at the base in exposures logged in ACI 5. The planar cross-bedded rudstone can only be observed in the northern sections (Figures 1B, 2, 4), overlain at the top of ACI 7 by trough cross-bedded rhodolith rudstones (Figure 2).
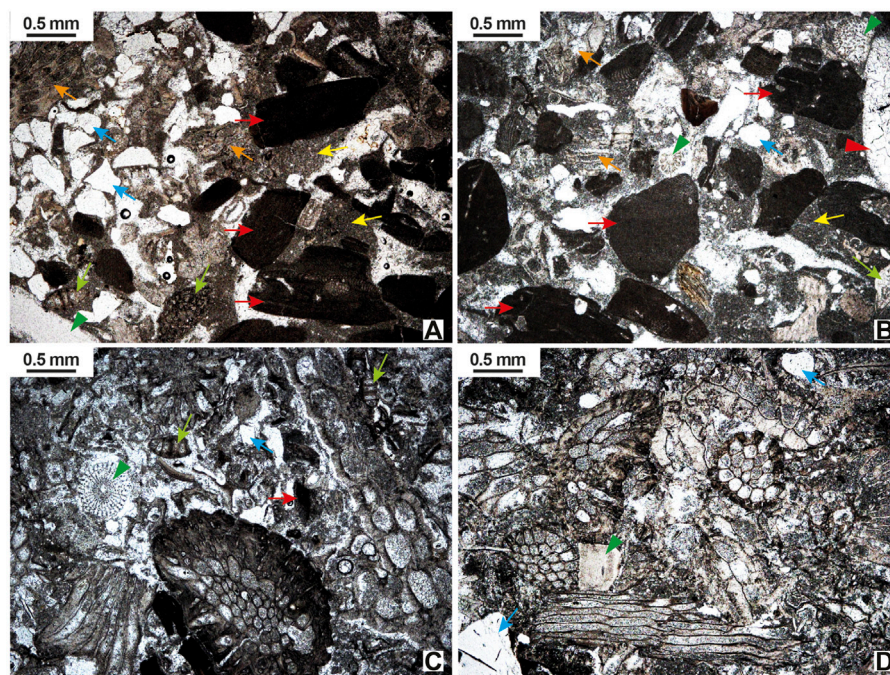
**FIGURE 5**
Micrographs of selected lithofacies in the Acinipo limestone. **(A)** Trough cross-bedded packstone to rudstone. Coralline algal fragments are the main components, followed by bryozoans (orange arrows). Benthic foraminifers (green arrows) and echinoids (green arrowheads) are secondary components. Quartz grains (blue arrows) are locally abundant. The matrix is commonly mudstone (yellow arrows). **(B)** Large-scale planar cross-bedded coralline rudstone. Coralline algae (red arrows), bryozoans (orange arrows), echinoids (green arrowheads), benthic foraminifers (green arrows), and terrigenous grains, mainly quartz (blue arrows) are the common components. Molds of aragonitic bivalves are filled with sparry calcite (red arrowhead). The matrix is a mudstone to wackestone (yellow arrow). **(C)** Large-scale planar cross-bedded bryozoan rudstone. Bryozoans are the main components with minor coralline algae (red arrows), echinoids (green arrowheads), benthic foraminifers (green arrows), and quartz (blue arrows). **(D)** Flat-bedded bryozoan packstone to rudstone. The rock is made of bryozoan fragments with echinoids (green arrowheads), benthic foraminifers (green arrows), terrigenous grains (blue arrows), and other bioclasts as very minor components.

# 6 Rhodolith size, morphology, and internal structure

Rhodoliths occur in well-lithified limestones, and they cannot be isolated from the cemented rock. Consequently, only 2D sections can be observed, preventing measuring their three axes. In addition, the length and width observable in sections are minimum values of the true rhodolith dimensions. Taking this into account, rhodoliths in Acinipo are up to 7.7 cm long, with a length median and mode of 4.5 cm (mean 4.6 cm and sd 1.2). The ratio width/length ranges from 0.43 to 0.96 (mean 0.68, median 0.68, and sd 0.12), indicating that they are flat ellipsoidal to spheroidal in shape. The shapes, however, are frequently hemi-ellipsoidal due to asymmetrical growth (see the following).

The rhodoliths are made up of encrusting to warty (very rarely fruticose) coralline algae (Figures 3A–D), intergrown with bryozoans and secondary serpulids, oysters, and encrusting foraminifers. The nuclei are bioclasts (bryozoans, mollusks, and coralline algal fragments) and less commonly lithoclasts. Rhodoliths bigger than 2.5 cm are usually multiphasic (Figure 3B). Coralline algae and other encrusters in the initial phase grew around a nucleus with a concentric arrangement; components of this initial phase were broken and abraded, and new coralline algae and invertebrates built a successive phase, which in turn was broken and overgrown by a third phase. These processes could be repeated several times, resulting in a complex boxwork arrangement, which can be strongly asymmetrical (Figure 3C). In some cases, fragments of two or more separate rhodoliths are bound together in a single nodule by coralline algae overgrowing them. In any phase, rhodoliths were bioeroded by sponges (*Entobia*), bivalves (*Gastrochaenolites*), and worms (*Trypanites*). The constructional and intraskeletal voids of encrusters and bioerosion traces are partially filled by mudstone to wackestone, locally including planktonic foraminifers. The remaining spaces are partially filled by sparry calcite cement.

**FIGURE 6**
Large-scale planar cross-bedded coralline algal rudstone at Section 7. Beds are dipping to the east.

# 7 Rhodolith-forming coralline algae

It is difficult to estimate the proportions of the coralline algae forming the rhodoliths in lithified rhodolith beds as any quantification of the relative abundance of components had to be carried out in a thin section under a microscope. The collection of rock samples and cutting of thin sections is conditioned by several factors that prevent a simple, random, or systematic sampling and, therefore, bias the results. In the rhodoliths analyzed in thin sections, *Lithophyllum* is the most common component, followed by Hapalidiales (*Lithothamnion* and *Mesophyllum*) and minor Corallinaceae (*Neogoniolithon* and *Spongites*) and *Sporolithon*.

*Lithophyllum* is represented by *L.* gr. *incrustans* Philippi 1837 (Figure 7A), *L.* gr. *dentatum* (Kützing) Foslie 1898, *L.* gr. *nitorum* W.H.Adey and P.J.Adey 1973 (Figure 7B), *L.* gr. *orbiculatum* (Foslie) Foslie 1900 (Figure 7C), *L.* gr. *pustulatum* (J.V.Lamouroux) Foslie 1906 (Figure 7F), and a possible specimen of *L.* gr. *hibernicum* Foslie 1906 (see Table 1 for characters separating the identified morphospecies groups).

*Lithothamnion ramosissimum* (Reuss) Piller 1994 is the most common species of the genus, with additional representatives of *L.* gr. *crispatum* Hauck 1878 (Figure 7D), and an unidentified species with large sporangial conceptacles (*Lithothamnion* sp. 1).

*Mesophyllum* is represented by one species that can be assigned to *M.* gr. *curtum* Lemoine 1939 (Figure 7E) and another two that cannot be confidently assigned to any

described species (*M.* sp. 1 and *M.* sp. 2, see Table 1 for characters separating them).

A species represented by a few specimens can be attributed to *Neogoniolithon* based on the coaxial arrangement of the hypothallus and uniporate sporangial conceptacles with columella. Only one plant can be assigned to *Spongites* gr. *fruticulosus* Kützing 1841, and two other small thalli show the characteristic sporangial compartments of *Sporolithon* (Figure 7F).

# 8 Depositional model

The extensive occurrence of trough cross-bedded rhodolith rudstones (Figures 2, 4) indicates that submarine dunes with rhodoliths and coralline algal gravel as main particle components covered most of the seafloor on which the Acinipo limestone formed (Figure 8). The dominance of *Lithophyllum* gr. *incrustans* and *Lithophyllum* gr. *dentatum* as components both in the inner and outer layers of rhodoliths from the base to the top of the sections indicates shallow depths of a few tens of meters for rhodolith growth during limestone accumulation. Both species are common in the shallowest 20 m, and their abundance rapidly decreases in deeper settings in the present-day western Mediterranean Sea (Braga et al., 2009; Del Río et al., 2022). *Lithophyllum* gr. *incrustans* is also the main component in the shallowest rhodoliths in the Pliocene of the Atlantic coast of Cádiz (Aguirre et al., 1993). The trough cross-bedded packstone
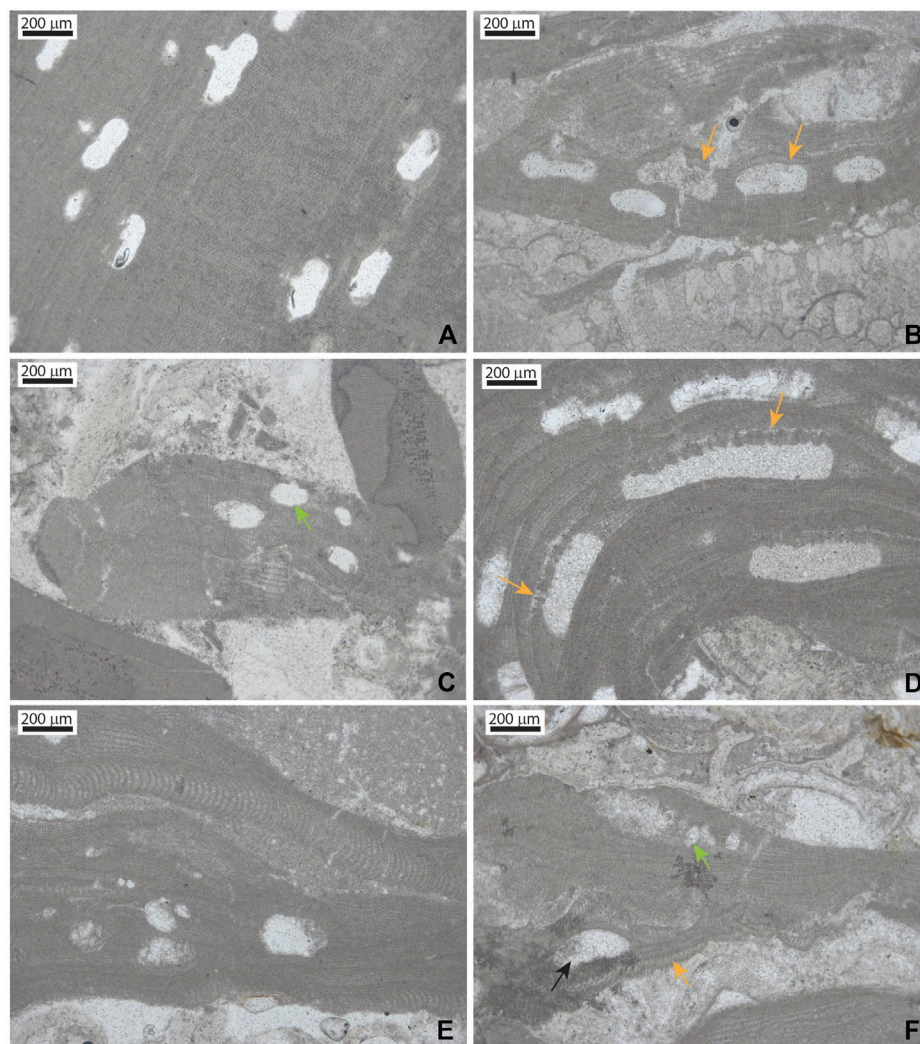
**FIGURE 7**
Micrographs of selected taxa in the coralline algal assemblages in the Acinipo limestone. **(A)** *Lithophyllum* gr. *incrustans*. Peripheral region with sporangial conceptacles. **(B)** *Lithophyllum* gr. *nitorum* growing on a bryozoan colony. Note the characteristic long cells in the conceptacle roof of the sporangial conceptacles. **(C)** Thallus fragment of *Lithophyllum* gr. *orbiculatum*. Note the small size of sporangial conceptacles (arrow) and the poor lateral alignment of cells of adjacent filaments. **(D)** Section of a short protuberance of *Lithothamnion* gr. *crispatum*. Note the characteristic pits in the sporangial conceptacle roof (arrows). **(E)** Thalli/branches of *Mesophyllum* gr. *curtum* with characteristic small-sized sporangial conceptacles with a hexagonal section. **(F)** *Lithophyllum* gr. *pustulatum* (orange arrow) and *Sporolithon* sp. with a sorus of sporangial compartments (green arrow).

to rudstone was probably a lateral variation of the trough cross-bedded rhodolith rudstones, in which breakage and abrasion of biogenic particles were higher.

The pervasive occurrence of large, angular to subrounded marly limestone clasts with low sphericity in the trough cross-bedded rudstones indicates proximity to the shoreline of the emergent basement. The majority of lithoclasts show *Gastrochaenolites* borings produced by bivalves. Large borings occur densely packed at any side of lithoclasts (Figure 3D), indicating that these remained for long periods on the seafloor by the shoreline before being incorporated into

submarine dunes. The lithoclast proportion is higher in the northwestern sections of the outcrop, which probably were closer to the shoreline. The base of section ACI 5 is a massive rudstone of lithoclasts and rhodoliths (Figure 2), which is probably the most proximal lithofacies in the Acinipo limestone. A similar conglomerate of broken, large rhodoliths and lithoclasts was described as a shallow water, nearshore facies in the upper-Tortonian fan-delta deposits in the Almanzora corridor (Braga and Martín, 1988). Although no well-defined sedimentary structures indicating tractive currents were observed in the massive conglomerate, the high degree of rhodolith

TABLE 1 Diagnostic characters separating the taxa recognized in the coralline algal assemblages in the Acinipo limestone. D= conceptacle diameter.

| | | |
|---|---|---|
| 1 sporangial compartment | | Sporolithales |
| 1 Multiporate sporangial conceptacles | | Hapalidiales |
| 1 Uniporate sporangial conceptacles | | Corallinales |
| Sporolithales | | *Sporolithon* sp. |
| Hapalidiales | | |
| 1 Plumose, non-coaxial ventral core | | *Lithothamnion* |
| *Lithothamnion* | 2 Pitted conceptacle roofs | *L.* gr. *crispatum* |
| | 2 Conceptacle roof without pits | 3 |
| | 3 Conceptacles concentrated in protuberances, D < 450 μm | *L. ramosissimum* |
| | 3 Conceptacles large, D > 600 μm, and thick conceptacle roof (50 μm) | *Lithothamnion* sp. 1 |
| 1 Coaxial ventral core | | *Mesophyllum* |
| *Mesophyllum* | 4 Conceptacle section polygonal, D < 400 μm | *M. curtum* |
| | 4 Conceptacle section elliptical, D > 400 μm | 5 |
| | 5 Conceptacle D < 700 μm | *Mesophyllum* sp. 1 |
| | 5 Conceptacles large, D > 700 μm | *Mesophyllum* sp. 2 |
| Corallinales | | |
| 1 Cell fusions | | Corallinaceae |
| | 2 Plumose, non-coaxial ventral core | *Spongites* gr. *fruticulosus* |
| | 2 Coaxial ventral core | *Neogoniolithon* sp. 1 |
| 1 Secondary pit connections | | Lithophyllacea |
| *Lithophyllum* | 3 Long, palisade cells in hypothallus | *L.* gr. *pustulatum* |
| | 3 Cells in hypothallus like those in perithallus | 4 |
| | 4 Long, palisade cells in the conceptacle roof | *L.* gr. *nitorum* |
| | 4 Cells in the conceptacle roof like those in perithallus | 5 |
| | 5 Cells of adjacent filaments well aligned | *L.* gr. *dentatum* |
| | 5 Poorly aligned cells of adjacent filaments | 6 |
| | 6 Long, cylindrical conceptacle pore | *L.* gr. *hibernicum* |
| | 6 Conical conceptacle pore | 7 |
| | 7 Conceptacles small, D < 200 μm | *L.* gr. *orbiculatum* |
| | 7 Conceptacle D > 200 μm | *L.* gr. *incrustans* |



FIGURE 8

Depositional model for the Acinipo limestone. Rhodoliths grew on a littoral wedge at the western side of the Ruinas de Acinipo bay. The wedge was affected by storms that incorporated the rhodoliths, other bioclasts, and lithoclasts from the basement into submarine dunes. Rhodoliths were broken but continued to grow on the dunes. Rhodoliths and bioclastic gravel were swept from the wedge top and accumulated on the foresets of the littoral wedge. Bryozoans dominate bioclasts in the distal portion of the foresets and in the open-platform deposits.

breakage and the large size of lithoclasts indicate reworking under high-energy conditions (Braga and Martín, 1988).

Large-scale planar cross-bedded rudstone in sections ACI 7 (Figure 5) and ACI 8 at the northern end of the Acinipo outcrop denotes deposition of successive beds on a steep slope dipping basinward and located immediately seaward of the submarine dunes. We interpret these beds as foresets of an infralittoral prograding wedge (Hernández-Molina et al., 2000), initially mainly fed by coralline algal gravel and sand-sized particles from the submarine dunes and later with higher proportions of bryozoan skeletons (Figure 8). The flat-bedded bryozoan packstone to rudstone in the isolated outcrop of section ACI 9 is the most distal and deeper deposit (Figure 8), now disconnected from the main outcrop.

Although the exposures do not allow precise measurements of many trough axes, cross-bedded sets indicate migration in several directions with predominant migration toward the north. This, together with the enclosed nature of the depositional setting (Gläser and Betzler, 2002), discards the existence of a persistent current strong enough to generate and move the coarse-grained submarine dunes. They are most probably formed by storm surges, mainly outflowing to N-NE. Storms affected the sediment mostly produced by coralline algae, which accumulated in an infralittoral wedge at the western side of a bay (the Ruinas de Acinipo bay of Gläser and Betzler, 2002). At the seaward front of the infralittoral wedge, bioclasts transported from its top by storm-generated return currents formed foresets below the mean storm wave base (Figure 8).

# 9 Discussion

## 9.1 Rhodoliths in storm-related deposits

The internal structure of large rhodoliths, showing several phases of repeated coralline algal growth and fragmentation/ erosion (Figure 3B), reflects their growth on a seafloor affected by storms. The edges of coralline thalli were broken and abraded during the removal and transport of rhodoliths by the storm surge. Once the rhodoliths settled on the seafloor, the thalli on the non-buried surface of rhodoliths re-started their growth or the surfaces were colonized by new thalli, during a period of quiescence long enough to allow the development of coralline algae and other encrusters. These processes took place several times in individual rhodoliths (Figure 3B) until their final burial within the dune deposits. Successive phases of fragmentation and re-started growth in multistory rhodoliths in the Middle Miocene carbonates from the Marion Plateau in northeastern Australia were interpreted as reflecting episodic storm reworking (Martín et al., 1993). A two-phase internal structure of Middle Miocene rhodoliths in the southern Apennines (Italy) was also considered by Checconi et al. (2010) as the result of offshore transport of the algal nodules by storm currents.

Rhodolith beds related to storms usually occur as broad, shallow channels filled with rhodoliths in deeper-middle ramp settings, which have been interpreted as storm surge channels. This is the case of the examples in the rhodolith pavement in the Upper Coralline Limestone Formation in Malta (Bosence and Pedley, 1982; Pedley, 1998) and in the Upper Miocene deposits in the Sorbas Basin in SE Spain (Puga-Bernabeu et al., 2007a). In the Malta pavement, however, rhodoliths also occur entrained in large-scale trough cross-bedding formed in submarine dunes. Orientation of foresets and rhodolith long axes indicate two or more current directions suggesting fluctuating energy conditions (Bosence and Pedley, 1982), characteristics of storm processes. According to Pedley (1998), cross-stratified deposits with abraded rhodoliths often occur in the shallowest Oligocene–Miocene rhodolith pavement facies in southern Italy and Malta. Trough cross-bedded intervals in the Pliocene rhodolith beds in Guadeloupe were also interpreted as formed by storms in the shallowest part of a middle ramp (Cornée et al., 2012).

In all these cases, rhodoliths and coralline algal gravel and sand-sized bioclasts are parautochthonous components entrained in submarine dunes on the seafloor. Rhodoliths might even be autochthonous if they grew immediately before the burial of the dune, as suggested by asymmetrical internal arrangements with predominantly upright growth in rhodoliths from the Acinipo limestone. In this limestone, although some siliciclastics and lithoclasts were incorporated into dune sediments, most components were carbonate skeletons produced on the western littoral wedge of the Ruinas de Acinipo bay.

The modern examples of rhodolith concentrations related to submarine dunes are substantially different from the Acinipo trough cross-bedded rhodolith rudstones. On the northeastern Brazilian shelf, rhodoliths grow in troughs of siliciclastic, large-scale submarine dunes and are probably incorporated together with bioclastic gravel in the base of the dunes (Testa and Bosence, 1998, 1999), but they are not their main components. Onshore of the sand-dune zone, rhodoliths grow at the crest and troughs of bioclastic sand ribbons parallel to the current direction. Rhodoliths and coralline gravel are incorporated into small and large wave ripples with crests roughly parallel to ribbon crests. These ripples are generated by waves approaching the coast, which is a flow system different from the one driving sand-ribbon movement (Testa and Bosence, 1999).

Storm deposits with rhodoliths described in the Macaronesian realm are also different from the Acinipo case. In Pleistocene tempestites from Maio (Cape Verde), rhodoliths occur within sand-sized deposits with swaley cross-stratification (Johnson et al., 2017). Hummocky and swaley cross-stratification in rhodolith-bearing packstones are also characteristics of Pleistocene storm deposits in Santiago (Cape Verde) (Johnson et al., 2012) and Miocene–Lower Pliocene tempestites from Santa Maria in the Azores archipelago (Johnson et al., 2017). Other

storm-related rhodolith concentrations in Cape Verde Islands are supratidal deposits resulting from the storm activity that transported the rhodoliths inland from their sites of growth or even from older fossil rhodolith beds (Johnson et al., 2017, 2020).

The large-scale planar cross-bedded coralline algal rudstone at the northern sections of the Acinipo outcrop (Figures 2, 6) is similar to the well-bedded rhodolith rudstone described by Brandano and Ronca, (2014) in the Miocene of northern Corsica. As in the Acinipo case, the dipping beds of the Corsican lithofacies accumulated in the foresets of a littoral wedge with rhodoliths fed from the top surface of the wedge and *in situ* growing coralline algae. The rhodolith floatstone that also occurs in the foresets of the littoral wedge in Corsica is rich in nodular bryozoans (Brandano and Ronca, 2014), which are the dominant components in the distal beds of large-scale planar cross-bedded rudstone in Acinipo. In the Corsican Miocene, however, on the top of the wedge, rhodoliths grew and accumulated in massive beds with only local planar cross-stratification (Brandano et al., 2009), instead of being pervasively incorporated into trough cross-beds.

## 9.2 Paleobiogeographical traits of the coralline algae

The coralline algal assemblages in the Acinipo rhodolith limestones are dominated by the Lithophyllaceae *Lithophyllum*, and Hapalidiales, with very minor occurrences of the Corallinaceae *Neogoniolithon* and *Spongites*. This composition reflects that the Ronda Basin was a marginal basin of the Guadalquivir Basin, which opened to the Atlantic Ocean. Similar components are reported from the Niebla Fm. in the western end of the Guadalquivir Basin in the only detailed account of Late Miocene coralline algae from this basin (Civis et al., 1994). *Lithophyllum* and Hapalidiales are also the only coralline algae in rhodoliths in the Pliocene of the Cádiz coast (Aguirre et al., 1993, 2017). The predominance of *Lithophyllum* among the Corallinales and the scarcity or absence of thick Corallinaceae is common in modern coralline assemblages in the Atlantic Iberian Peninsula (Lugilde et al., 2016) and in general in the European Atlantic coasts (Irvine and Chamberlain, 1994), and contrasts with a higher abundance of *Neogoniolithon* and *Spongites* in the Mediterranean Sea (Rindi et al., 2019). However, *Neogoniolithon brassica-florida* (Harvey) Setchell and Mason 1943, is locally abundant in *Cymodocea* seagrass meadows in the Bay of Cadiz (Bermejo et al., 2012; Hernández-Kartun et al., 2015). The tendency of thick Corallinaceae to inhabit warmer waters was already recorded in the Late Miocene coralline assemblages in southern Spain. *Neogoniolithon*, *Spongites*, and *Lithoporella* were common during periods of coral reef growth in the Betic Neogene

basins, whereas they were scarce or absent during periods of deposition of heterozoan, warm-temperate carbonates (Braga and Aguirre, 2001). In contrast, *Lithophyllum* is common in these heterozoan carbonates, and most species groups found in the Ronda Basin (*L. incrustans*, *L. dentatum*, *L. nitorum*, *L. orbiculatum*, and *L. pustulatum*) were recorded in the Betic Neogene Mediterranean-linked basins (Braga and Aguirre, 1995, 2001; Puga-Bernabeu et al., 2007a; Puga-Bernabeu et al., 2007b).

## Data availability statement

The raw data supporting the conclusion of this article will be made available by the authors, without undue reservation.

## Author contributions

JB and JA shared the research design, fieldwork, taxonomic identification, and writing the manuscript.

## Conflict of interest

The authors declare that the research was conducted in the absence of any commercial or financial relationships that could be construed as a potential conflict of interest.

## Publisher's note

All claims expressed in this article are solely those of the authors and do not necessarily represent those of their affiliated organizations, or those of the publisher, the editors, and the reviewers. Any product that may be evaluated in this article, or claim that may be made by its manufacturer, is not guaranteed or endorsed by the publisher.

# References

Adey, W. H., and Adey, P. J. (1973). Studies on the biosystematics and ecology of the epilithic crustose Corallinaceae of the British Isles. *Br. Phycol. J.* 8, 343–407. doi:10.1080/00071617300650381

Aguirre, J., Braga, J. C., and Bassi, D. (2017). "Rhodoliths and rhodolith beds in the rock record," in *Rhodolith/maërl beds: A global perspective*. Editors R. Riosmena-Rodríguez, W. Nelson, and J. Aguirre (Basel: Springer Inter. Publ.), 105–138. doi:10.1007/978-3-319-29315-8_5

Aguirre, J., Braga, J. C., and Martín, J. M. (1993). "Algal nodules in the upper Pliocene deposits at the coast of Cadiz (S Spain)," in *Studies on fossil benthic algae*. Editors F. Barattolo, P. De Castro, and M. Parente (Rome: Boll. Soc. Paleontol. It.), Vol. 1, 1–7.

Aguirre, J., Braga, J. C., Martín, J. M., and Betzler, C. (2012). Palaeoenvironmental and stratigraphic significance of Pliocene rhodolith beds and coralline algal bioconstructions from the Carboneras Basin (SE Spain). *Geodiversitas* 34, 115–136. doi:10.5252/g2012n1a7

Balanyá, J. C., Crespo-Blanc, A., Díaz Azpiroz, M., Expósito, I., and Luján, M. (2007). Structural trend line pattern and strain partitioning around the Gibraltar arc accretionary wedge: Insights as to the mode of orogenic arc building. *Tectonics* 26, TC2005. doi:10.1029/2005TC001932

Barnolas, A., Larrasoaña, J. C., Pujalte, V., Schmitz, B., Sierro, F. J., Mata, M. P., et al. (2019). "Alpine foreland basins," in *The geology of iberia: A geodynamic approach*. Editors C. Quesada, and J. T. Oliveira (Cham: Springer), 7–59. doi:10.1007/978-3-030-11190-8_2

Bassi, D., and Nebelsick, J. H. (2010). Components, facies and ramps: Redefining Upper Oligocene shallow water carbonates using coralline red algae and larger foraminifera (Venetian area, northeast Italy). *Palaeogeogr. Palaeoclimatol. Palaeoecol.* 295, 258–280. doi:10.1016/j.palaeo.2010.06.003

Benisek, M.-F., Betzler, C., Marcano, G., and Mutti, M. (2009). Coralline-algal assemblages of a burdigalian platform slope: Implications for carbonate platform reconstruction (northern Sardinia, Western Mediterranean Sea). *Facies* 55, 375–386. doi:10.1007/s10347-009-0183-7

Benisek, M.-F., Marcano, G., Betzler, C., and Mutti, M. (2010). "Facies and stratigraphic architecture of a Miocene warm-temperate to tropical fault-block carbonate platform, Sardinia (central Mediterranean Sea)," in *Carbonate Syst. Dur. Oligocene-Miocene Clim. Transition.* Editors M. Mutti, W. E. Piller, and C. Betzler (Chichester; Hoboken, NJ: IAS Spec. Publ Wiley-Blackwell), 42, 107–128.

Bermejo, R., Pérez-Llorens, J. L., Vergara, J., and Hernández, I. (2012). Notas corológicas del macrofitobentos marino de Andalucía (España). X. New records for the seaweeds of Andalusia (Spain). X. *Acta Botanica Malacitana* 37, 163–165. doi:10.24310/abm.v37i0.2660

Betzler, C., Braga, J. C., Martín, J. M., Sánchez-Almazo, I. M., and Lindhorst, S. (2006). Closure of a seaway: Stratigraphic record and facies (Guadix basin, southern Spain). *Int. J. Earth Sci. (Geol. Rundschau)* 95, 903–910. doi:10.1007/s00531-006-0073-y

Bosence, D. W. J., and Pedley, H. M. (1982). Sedimentology and palaeoecology of a Miocene coralline algal biostrome from the Maltese Islands. *Palaeogeogr. Palaeoclimatol. Palaeoecol.* 38, 9–43. doi:10.1016/0031-0182(82)90062-1

Bourgois, J. (1978). La transversale de Ronda (cordillères bétiques, espagne). Besançon: University of Besançon. PhD Thesis.

Braga, J. C., and Aguirre, J. (2001). Coralline algal assemblages in upper Neogene reef and temperate carbonates in Southern Spain. *Palaeogeogr. Palaeoclimatol. Palaeoecol.* 175, 27–41. doi:10.1016/S0031-0182(01)00384-4

Braga, J. C., Aguirre, J., and Esteban, J. (2009). Calcareous algae of Cabo de gata-níjar nature park. Field guide, *ACUMED y* consejería *de Medio ambiente.* Madrid: Junta de Andalucía.

Braga, J. C., and Aguirre, J. (1995). Taxonomy of fossil coralline algal species: Neogene Lithophylloideae (Rhodophyta, Corallinaceae) from southern Spain. *Rev. Palaeobot. Palynology* 86, 265–285. doi:10.1016/0034-6667(94)00135-7

Braga, J. C., and Martín, J. M. (1988). Neogene coralline-algal growth-forms and their palaeoenvironments in the Almanzora river valley (almeria, S.E. Spain). *Palaeogeogr. Palaeoclimatol. Palaeoecol.* 67, 285–303. doi:10.1016/0031-0182(88)90157-5

Brandano, M., Frezza, V., Tomassetti, L., Pedley, M., and Matteucci, R. (2009). Facies analysis and palaeoenvironmental interpretation of the late Oligocene attard member (lower coralline Limestone Formation), Malta. *Sedimentology* 56, 1138–1158. doi:10.1111/j.1365-3091.2008.01023.x

Brandano, M. (2017). "Oligocene rhodolith beds in the central Mediterranean area," in *Rhodolith/maërl beds: A global perspective*. Editors R. Riosmena-Rodríguez, W. Nelson, and J. Aguirre (Basel: Springer Inter. Publ), 195–219. doi:10.1007/978-3-319-29315-8_8

Brandano, M., and Piller, W. E. (2010). "Coralline algae, oysters and echinoids – A liaison in rhodolith formation from the burdigalian of the latium-abruzzi platform (Italy)," in *Carbonate systems during the Oligocene-Miocene climatic transition*. Editors M. Mutti, W. E. Piller, and C. Betzler (Chichester; Hoboken, NJ: IAS Spec. Publ. Wiley-Blackwell), 42, 149–164.

Brandano, M., and Ronca, S. (2014). Depositional processes of the mixed carbonate-siliciclastic rhodolith beds of the Miocene Saint-Florent Basin, northern Corsica. *Facies* 60, 73–90. doi:10.1007/s10347-013-036710.1007/s10347-013-0367-z

Brandano, M., Vannucci, G., Pomar, L., and Obrador, A. (2005). Rhodolith assemblages from the lower tortonian carbonate ramp of Menorca (Spain): Environmental and paleoclimatic implications. *Palaeogeogr. Palaeoclimatol. Palaeoecol.* 226, 307–323. doi:10.1016/j.palaeo.2005.04.034

Checconi, A., Bassi, D., Carannante, P., and Monaco, G. (2010). Re-Deposited rhodoliths in the middle Miocene hemipelagic deposits of vitulano (southern Apennines, Italy): Coralline assemblage characterization and related trace fossils. *Sediment. Geol.* 225, 50–66. doi:10.1016/j.sedgeo.2010.01.001

Civis, J., Alonso-Gavilan, G., Gonzalez-Delgado, J. A., and Braga, J. C. (1994). Sédimentation carbonatée transgressive sur la bordure occidentale du couloir nord-bétique pendant le Tortonien supérieur (Fm Calcarenita de Niebla, SW de l'Espagne). *Géol. Méditerr.* 21, 9–18. doi:10.3406/geolm.1994.1493

Cornée, J. J., Léticée, J. L., Münch, P., Quillévéré, F., Lebrun, J. F., Moissette, P., et al. (2012). Sedimentology, palaeoenvironments and biostratigraphy of the Pliocene-Pleistocene carbonate platform of Grande-Terre (Guadeloupe, Lesser Antilles forearc). *Sedimentology* 59, 1426–1451. doi:10.1111/j.1365-3091.2011.01311.x

Del Río, J., Ramos, D. A., Sánchez-Tocino, L., Peñas, J., and Braga, J. C. (2022). The punta la Mona rhodolith bed: Shallow-water mediterranean rhodoliths (almuñecar, granada, southern Spain). *Front. Earth Sci.* 10, 884685. doi:10.3389/feart.2022.884685

Fernàndez, M., Berástegui, X., Puig, C., Garcia-Castellanos, D., Jurado, M. J., Torné, M., et al. (1998). "Geophysical and geological constraints on the evolution of the Guadalquivir foreland basin, Spain," in *Cenozoic Forel. Basins West. Eur.* Editors A. Mascle, C. Puigdefàbregas, H. P. Luterbacher, and M. Fernàndez (London: Geological Society Special Publication), 134, 29–48.

Foslie, M. (1906). Algologiske notiser II. *Det. K. Nor. Vidensk. Selsk. Skr.* 1906 (2), 1–28.

Foslie, M. (1898). List of species of the lithothamnia. *K. Nor. Vidensk. Selsk. Skr.* 1898 (3), 1–11.

Foslie, M. (1900). Revised systematical survey of the Melobesieae. *K. Nor. Vidensk. Selsk. Skr.* 1900 (5), 1–22.

Galindo-Zaldívar, J., Braga, J. C., Marín-Lechado, C., Ercilla, G., Martín, J. M., Pedrera, A., et al. (2019). "Extension in the western mediterranean," in *The geology of iberia: A geodynamic approach*. Editors C. Quesada, and J. T. Oliveira (Cham: Springer), 61–103. doi:10.1007/978-3-030-11190-8_3

Garcia-Castellanos, D., Fernàndez, M., and Torne, M. (2002). Modeling the evolution of the Guadalquivir foreland basin (southern Spain). *Tectonics* 21, 9–1. doi:10.1029/2001TC001339

Gläser, I., and Betzler, C. (2002). Facies partitioning and sequence stratigraphy of cool-water, mixed carbonate-siliciclastic sediments (Upper Miocene Guadalquivir Domain, southern Spain). *Int. J. Earth Sci. (Geol. Rundschau)* 91, 1041–1053. doi:10.1007/s00531-002-0293-8

Hauck, F. (1878). Beiträge zur Kenntniss der adriatischen Algen. *Osterr. Bot. Z.* 28, 288–295. doi:10.1007/bf01614959

Hernández-Kantún, J., Riosmena-Rodriguez, R., Hall-Spencer, J. M., Peña, V., Maggs, C., and Rindi, F. (2015). Phylogenetic analysis of rhodolith formation in the Corallinales (Rhodophyta). *Eur. J. Phycol.* 50, 46–61. doi:10.1080/09670262.2014.984347

Hernández-Molina, J., Fernández-Salas, L. M., Lobo, F. J., and Somoza, L. (2000). The infralittoral prograding wedge: A new large-scale progradational sedimentary body in shallow marine environments. *Geo-Marine Lett.* 20, 109–117. doi:10.1007./s003670000040

Iribarren, L., Vergés, J., and Fernàndez, M. (2009). Sediment supply from the Betic-Rif orogen to basins through Neogene. *Tectonophysics* 475, 68–84. doi:10.1016/j.tecto.2008.11.029

Irvine, L. M., and Chamberlain, Y. M. (1994). *Seaweeds of the British isles. Volume I. Rhodophyta. Part 2B. Corallinales, Hildebrandiales*. London: The Natural History Museum.

Jeong, S. Y., Nelson, W. A., Sutherland, J. E., Peña, V., Le Gall, L., Diaz-Pulido, G., et al. (2021). Corallinapetrales and corallinapetraceae: A new order and new family

of coralline red algae including *Corallinapetra gabriellii* comb. Nov. *J. Phycol* 57, 849–862. doi:10.1111/jpy.13115-20-107

Johnson, M. E., Baarli, G. B., Cachão, M., da Silva, C. M., Ledesma-Vázquez, J., Mayoral, E. J., et al. (2012). Rhodoliths, uniformitarianism, and Darwin: Pleistocene and Recent carbonate deposits in the Cape Verde and Canary archipelagos. *Palaeogeogr. Palaeoclimatol. Palaeoecol.* 329-330, 83–100. doi:10.1016/j.palaeo.2012.02.019

Johnson, M. E., Ledesma-Vázquez, J., Ramalho, R. S., da Silva, C. M., Rebelo, A., Santos, G. B., et al. (2017). "Taphonomic range and sedimentary dynamics of modern and fossil rhodolith beds: Macaronesian realm (North Atlantic Ocean)," in *Rhodolith/maërl beds: A global perspective*. Editors R. Riosmena-Rodríguez, W. Nelson, and J. Aguirre (Basel: Springer Inter. Publ.), 221–261. doi:10.1007/978-3-319-29315-8_9

Johnson, M. E., Ramalho, R. S., and Marques da Silva, C. M. (2020). Storm-related rhodolith deposits from the upper Pleistocene and recycled coastal holocene on sal island (cabo Verde archipelago). *Geosciences* 10, 419. doi:10.3390/geosciences10110419

Kützing, F. T. (1841). *Über die 'Polypiers calcifères' des Lamouroux*. Nordhausen, F. Thiele, 34.

Lemoine, M. P. (1939). Les algues calcaires fossiles de l'Algérie. *Matériaux Carte Géologique L'Algérie. 1re. Série Paléontologie* 9, 1–128.

Lirer, F., Foresi, L. M., Iaccarino, S. M., Salvatorini, G., Turco, E., Cosentino, C., et al. (2019). Mediterranean Neogene planktonic foraminifer biozonation and biochronology. *Earth-Science Rev.* 196, 102869. doi:10.1016/j.earscirev.2019.05.013

Lugilde, J., Peña, V., and Bárbara, I. (2016). The order Corallinales sensu lato (rhodophyta) in the iberian atlantic: Current state of knowledge. *Anal. Jard. Bot. Madrid* 73, 038. doi:10.3989/ajbm.2424

Martín, J. C., Braga, J. C., Aguirre, J., and Puga-Bernabéu, Á. (2009). History and evolution of the north-Betic strait (prebetic zone, betic cordillera): A narrow, early tortonian, tidal-dominated, atlantic-mediterranean marine passage. *Sediment. Geol.* 216, 80–90. doi:10.1016/j.sedgeo.2009.01.005

Martin, J. M., Braga, J. C., and Betzler, C. (2001). The messinian guadalhorce corridor: The last northern, atlantic-mediterranean gateway. *Terra nova.* 13, 418–424. doi:10.1046/j.1365-3121.2001.00376.x

Martín, J. M., Braga, J. C., Konishi, K., and Pigram, C. J. (1993). A model for the development of rhodoliths on platforms influenced by storms: Middle Miocene carbonates of the Marion Plateau (northeastern Australia). *Proc. Ocean Drill. Program, Sci. Results* 133, 455–460.

Martín, J. M., Puga-Bernabéu, Á., Aguirre, J., and Braga, J. C. (2014). Miocene atlantic-mediterranean seaways in the betic cordillera (southern Spain). *Rev. Soc. Geol. Esp.* 27, 175–186.

Martini, E. (1971). Standard Tertiary and Quaternary calcareous nannoplankton zonation. *Proc. 2nd Int. Conf. Plankton* Vol. 2, 739–785.

Millar, K. R., and Gagnon, P. (2018). Mechanisms of stability of rhodolith beds: Sedimentological aspects. *Mar. Ecol. Prog. Ser.* 594, 65–83. doi:10.3354/meps12501

Nalin, R., Nelson, C. S., Basso, D., and Massari, F. (2008). Rhodolith-bearing limestones as transgressive marker beds: Fossil and modern examples from north island, New Zealand. *Sedimentology* 55, 249–274. doi:10.1111/j.1365-3091.2007.00898.x

Obrador, A., Pomar, L., and Taberner, C. (1992). Late Miocene breccia of Menorca (balearic Islands) a basis for the interpretation of a Neogene ramp deposit. *Sediment. Geol.* 79, 203–223. doi:10.1016/0037-0738(92)90012-G

Okada, H., and Bukry, D. (1980). Supplementary modification and introduction of code numbers to the low-latitude coccolith biostratigraphic zonation (Bukry, 1973; 1975). *Mar. Micropaleontol.* 5, 321–325. doi:10.1016/0377-8398(80)90016-x

Pedley, H. M. (1998). "A review of sediment distributions and processes in Oligo-Miocene ramps of southern Italy and Malta (Mediterranean divide)," in *Carbonate ramps*. Editors V. P. Wrigh, and T. P. Burchette (London: Geol. Soc. London Spec. Publ.), 149, 163–179. doi:10.1144/gsl.sp.1999.149.01.09

Peña, V., Vieira, C., Braga, J. C., Aguirre, J., Rösler, A., Baele, G., et al. (2020). Radiation of the coralline red algae (Corallinophycidae, Rhodophyta) crown group as inferred from a multilocus time-calibrated phylogeny. *Mol. Phylogenetics Evol.* 150, 106845. doi:10.1016/j.ympev.2020.106845

Philippi, R. (1837). Beweiss dass die Nulliporen Pflanzen sind. *Arch. für Naturgeschichte* 3, 387–393.

Piller, W. E. (1994). *Nullipora ramosissima* REUSS, 1847--a rediscovery. *Beitr. Paläontol.* 19, 181–189.

Pisera, A., and Studencki, W. (1989). Middle Miocene rhodoliths from the korytnica basin (southern Poland): Environmental significance and paleontology. *Acta palaeont. Pol.* 34, 179–209.

Pomar, L., Obrador, A., and Westphal, H. (2002). Sub-wavebase cross-bedded grainstones on a distally steepened carbonate ramp, upper Miocene, Menorca, Spain. *Sedimentology* 49, 139–169. doi:10.1046/j.1365-3091.2002.00436.x

Pomar, L. (2001). Types of carbonate platforms: A genetic approach. *Basin Res.* 13, 313–334. doi:10.1046/j.0950-091x.2001.00152.x

Puga-Bernabéu, Á., Braga, J. C., Aguirre, J., and Martín, J. M. (2022). Sedimentary dynamics and topographic controls on the tidal-dominated zagra strait, early tortonian, betic cordillera, Spain. *Geol. Soc. Lond. Spec. Publ.* 523, 85. doi:10.1144/SP523-2021-85

Puga-Bernabéu, Á., Braga, J. C., and Martín, J. M. (2007a). High-frequency cycles in upper-miocene ramp-temperate carbonates (Sorbas Basin, SE Spain). *Facies* 53, 329–345. doi:10.1007/s10347-007-0107-3

Puga-Bernabéu, Á., Martín, J. M., and Braga, J. C. (2007b). Tsunami-related deposits in temperate carbonate ramps, Sorbas basin, southern Spain. *Sediment. Geol.* 199, 107–127. doi:10.1016/j.sedgeo.2007.01.020

Raffi, I., and Flores, J. A. (1995). Pleistocene through Miocene calcareous nannofossils from eastern equatorial pacific ocean (leg 138). *Proc. Ocean Drill. Program, Sci. Results* 138, 233–286. doi:10.2973/odp.proc.sr.138.112.1995

Rindi, F., Braga, J. C., Martin, S., Peña, V., Le Gall, L., Caragnano, A., et al. (2019). Coralline algae in a changing Mediterranean Sea: How can we predict their future, if we do not know their present? *Front. Mar. Sci.* 6, 723. doi:10.3389/fmars.2019.00723

Rodríguez-Fernández, J. (1982). El Mioceno del sector central de las Cordilleras Béticas. Granada: Publ. Univ. Granada, 202. Tesis Doctoral.

Ruiz-Constán, A., Galindo-Zaldívar, J., Pedrera, A., and de Galdeano, C. (2009). Gravity anomalies and orthogonal box fold development on heterogeneous basement in the Neogene Ronda Depression (Western Betic Cordillera). *J. Geodyn.* 47, 210–217. doi:10.1016/j.jog.2008.09.004

Serrano, F. (1979). Los foraminíferos planctónicos del Mioceno superior de la cuenca de Ronda y su comparación con los de otras áreas de la Cordilleras Béticas. Málaga: Univ. Málaga, 272. PhD Thesis.

Setchell, W. A., and Mason, L. R. (1943). Goniolithon and Neogoniolithon. *Proc. Natl. Acad. Sci. U.S.A.* 29, 87–92. doi:10.1073/pnas.29.3-4.87

Sierro, F. J. (1985). The replacement of the"Globorotalia menardii" group by theGloborotalia miotumida group: An aid to recognizing the Tortonian-Messinian boundary in the Mediterranean and adjacent Atlantic. *Mar. Micropaleontol.* 9, 525–535. doi:10.1016/0377-8398(85)90016-7

Sola, F., Braga, J. C., and Sælen, G. (2022). Contradictory coeval vertical facies changes in upper Miocene heterozoan carbonate-terrigenous deposits (Sierra de Gádor, Almería, SE Spain). *J. Sediment. Res.* 92, 257–274. doi:10.2110/jsr.2022.010

Testa, V., and Bosence, D. W. J. (1998). "Carbonate-siliciclastic sedimentation on a high-energy, ocean-facing, tropical ramp, NE Brazil," in *Carbonate ramps*. Editors V. P. Wrigh, and T. P. Burchette (London: Geol. Soc. London Spec. Publ.), 149, 55–71. doi:10.1144/gsl.sp.1999.149.01.05

Testa, V., and Bosence, D. W. J. (1999). Physical and biological controls on the formation of carbonate and siliciclastic bedforms on the north-east Brazilian shelf. *Sedimentology* 46, 279–301. doi:10.1046/j.1365-3091.1999.00213.x

Vergés, J., and Fernàndez, M. (2012). Tethys-Atlantic interaction along the Iberia-Africa plate boundary: The Betic-Rif orogenic system. *Tectonophysics* 579, 144–172. doi:10.1016/j.tecto.2012.08.032

Woelkerling, W. J., Irvine, L. M., and Harvey, A. S. (1993). Growth-forms in non-geniculate coralline red algae (coralliinales, rhodophyta). *Aust. Syst. Bot.* 6, 277–293. doi:10.1071/sb9930277

Young, J. R., Flores, J. A., and Wei, W. (1994). A summary chart of Neogene nannofossil magnetobiostratigraphy. *J. Nannoplankt. Res.* 16, 21–27.